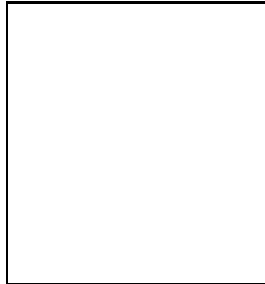


Accretion, star formation and relativistic particles in AGN number 1

S. Nayakshin

*Max Planck Institut fr Astrophysik
Karl-Schwarzschild-Str. 1 85741 Garching, Germany*



Sgr A* is the $\simeq 3 \times 10^6 M_\odot$ supermassive black hole (SMBH) in the Center of our Galaxy, famous for its low luminosity. While this fact makes it hard to observe Sgr A* at any frequency, it also allows relativistic particles to avoid cooling. We briefly review the evidence that Sgr A* is surrounded by two-temperature semi-relativistic plasma with a possible small admixture of non-thermal electrons. During the X-ray flares, the non-thermal component seems to gain prominence. We then turn to processes operating on larger scales, e.g. ~ 0.1 parsec away from Sgr A* that control its current feeding and the relatively recent star formation history. We show that the initial total mass of the two young stellar disks observed to exist in Sgr A* could not have exceeded about $\sim 2 \times 10^4 M_\odot$ if the stars were formed via self-gravity in a massive accretion disk. On the other hand, if the stars belonged to a massive star cluster that spiraled in due to dynamical friction, the mass limit becomes a factor of few lower. Finally, we describe our recent results and outlook on the numerical simulations of stellar winds accreting onto Sgr A*. The main result we wish to emphasize are the large variability in the accretion pattern on the SMBH on time scales of hundreds and thousands of years due to changes in the configuration of stellar orbits. This implies that, averaged on time scales of thousands of years, Sgr A* may be orders of magnitude more luminous in all wavebands, and especially in the X-ray and γ -ray bands, than its current meager luminosity. Thus Sgr A*'s role for the energy balance of the gas, including relativistic particles, in the inner Galaxy may be quite significant.

1 Introduction

Sgr A* is believed to be the $M_{\text{BH}} \simeq 3.5 \times 10^6 M_\odot$ super-massive black hole (SMBH) in the very centre of our Galaxy^{41,14}. Since any other SMBH residing in a center of a galaxy is at least a factor of a hundred farther away from us than Sgr A*, the latter can be safely called the “AGN number 1”. Studying the center of our Galaxy should yield clues to Physics and Astrophysics of SMBH in general.

In this paper we shall touch upon three sides of our current understanding of Sgr A* – the physics of the accretion flow in the inner few hundred Schwarzschild radii, then that at much larger radii where winds from young massive stars are captured into the accretion flow proper, and finally the recent history of star formation near Sgr A*.

2 Inefficient accretion and hot plasma

This conference is devoted to very high energy particles in the Universe. Black holes are in principle capable of accelerating particles to relativistic energies as their gravitational potential is quite deep. However in practice there can be a number of cooling processes damping production of relativistic particles. Although this is not directly obvious from theoretical arguments as the accretion flow geometry in general is not well constrained, observations suggest a somewhat ironical situation for high energy relativistic particles in AGN, in which Sgr A* occupies an important place. In high luminosity, high accretion rate AGN, reviewed at this meeting by B. Czerny, prevalence of relativistic particles seems to be limited to jets. The high energy emission of the latter is usually hard to observe because it is beamed away from us except for blazars where jets point almost directly to us. In fact, bolometrically, most of bright AGN emission is emitted in the optical-UV regions, implying that accretion disks there have temperatures of order $T \sim 10^5 K$. The high energy spectra of accretion flows in luminous AGN do extend to high energies, but “only” to photon energies of about 100 keV, with hints of thermal roll-overs observed in many AGN (see B. Czerny’s contribution). This means that the bulk of particles even in the hottest regions of the accretion flow, such as X-ray emitting coronae, are thermal, and have temperature no larger than $T \sim 100 keV$ or $\sim 10^9$ Kelvin.

On the other hand, in low luminosity, low accretion rate AGN, the inner regions of accretion flows appear to be much hotter than $T \sim 10^5 K$ because the thermal-like disk spectrum is characteristically absent in these objects⁴³. The most straight forward explanation to this fact is to assume that at some critical accretion rate there is a transition from the radiatively efficient (high luminosity AGN³⁹) to radiatively-inefficient accretion modes^{27,28}. As implied by the name, while gaining energy due to falling in a deep potential well, gas in these accretion flows does not cool efficiently enough to remain cold as in the bright AGN. This is a great news for production of relativistic particles, but at the same time it also means that these hot accretion flows are hard to observe exactly because they radiate little.

2.1 Quiescent accretion onto Sgr A*

Sgr A* is a champion “under-achiever” among low luminosity AGN (LLAGN). Because of this fact, and due to its proximity, observations of Sgr A* are extremely important for the whole class of LLAGN. The evidence for a hot, non-radiative flow onto Sgr A* comes from amismatch between the inferred accretion rate onto the SMBH and the observed bolometric luminosity. In particular, the Bondi accretion rate onto Sgr A* is estimated¹ at $\sim 10^{-6} M_{\odot} \text{ year}^{-1}$ at $\sim 10^5 R_S$ distances from the SMBH. Further in, at distances of order few hundred R_S , linear polarization measurements at a range of radio wavelengths constrain⁴ the accretion rate onto the SMBH to a value of $\sim 10^{-8} - 10^{-7} M_{\odot} \text{ year}^{-1}$. Even with the lowest accretion rate estimate one would expect Sgr A* to be as bright as $\sim 10^{38} \text{ erg/sec}$, whereas the bolometric luminosity of Sgr A* reaches²⁸ only $\sim 3 \times 10^{36} \text{ erg/sec}$.

It appears that the only reasonable way out of the radiation output discrepancy is to assume that electrons are not well coupled to ions via Coulomb collisions⁴⁰, and that therefore they radiate much less than they would in a one-temperature model. However there is also the discrepancy in the accretion rates at small and large radii, and that is explained as another consequence of the gas being unable to cool. Namely, viscous or convective heating of the gas,

in the absence of radiative cooling, unbinds much of the gas, severely reducing the accretion rate^{3,36}. Most of electrons are expected to be thermal due to thermalisation via synchrotron self-absorption, whereas protons may be in principle be non-thermal²². Detailed spectral fits support these ideas, although it must be noted that an energetically small non-thermal component to the electron distribution function would actually explain the otherwise unexplained detailed shape of the low frequency radio spectrum⁴⁴.

A bright O-type star with bolometric luminosity of about 10^5 Solar luminosities passed only $\sim 2000R_S$ away from Sgr A* in 2002^{41,14}. Semi-relativistic electrons in the accretion flow would up-scatter the optical emission into X-rays and gamma-rays, which in principle can be observed. Moreover, since Chandra observations during 2002 luckily covered the peri-center passage of S2, and no Sgr A* brightening in X-rays was seen, one can set a limit³¹ on the accretion rate of about $\lesssim 3 \times 10^{-7} M_\odot/\text{year}$. This limit is independent of the linear polarization measurements in the radio, and is sensitive to electrons somewhat closer in to the SMBH, at tens of Schwarzschild radii.

2.2 Flaring states of Sgr A*: non-thermal particles

The story of Sgr A* does not end with its mysteriously tiny quiescent emission. The source also emits short duration X-ray and near-infrared (NIR) flares^{2,11}. The flares last from 2 to ~ 20 thousand seconds, seem to repeat every day or so, and vary in intensity from barely detectable on the level of the quiescent emission to as bright as ~ 100 times the quiescent luminosity³⁵.

The author of this paper suggested²⁹ that the X-ray flares may actually be coming not from Sgr A* itself but from stars colliding with a yet unseen cold accretion disk perhaps existing on $\sim 0.1''$ scales from Sgr A*. However, observed later¹¹, the NIR flares come from a much closer vicinity of Sgr A*, with evidence for a linear polarization in at least one NIR flare. Among other theoretical suggestions, a sudden density change in the relativistic disk model²¹ appears to be also too finely tuned.

The most likely origin for the X-ray/NIR flares is either a jet²³ or the inner part of the accretion flow⁴⁴ in Sgr A*. Among possible variations in the jet/accretion flow structure, variations in the particle density or magnetic field strength are disfavored²³, because these would predict rapid variability in the radio emission of Sgr A*, which has not yet been observed. Variations in the high energy tail of the electron particle distribution function appear to explain the X-ray/NIR flares much more naturally^{23,44}. Summarizing, it appears that accretion and/or jet in Sgr A* in quiescence contains mainly thermal electrons with $T \lesssim 10^{11}$ Kelvin, with only a small admixture of non-thermal power law. However during the flares the non-thermal component becomes much more prominent. A detailed understanding of acceleration processes, time scales for the events, and energetics is nevertheless missing.

3 Wind feeding simulations

To understand what happens in the last few Schwarzschild radii of a SMBH, we need to solve gas dynamics from large to small radii. Unfortunately, we do not have good observational constraints on the origin of gas accreting on to the SMBHs in external galaxies. Therefore AGN accretion discs are less well understood than discs in X-ray binaries on comparable relative scales. Sgr A* is the only exception to this as we can directly observe stellar winds and ionized gas motions as close as ~ 0.1 parsec to the SMBH. From *Chandra* observations of the Galactic centre region, one can measure¹ the gas density and temperature around the inner arcsecond and then estimate the Bondi accretion rate of $\dot{M} \sim 10^{-6} M_\odot \text{ year}^{-1}$. However, unlike in the classical textbook problem of Bondi accretion, hot gas is continuously created in shocked winds expelled by tens of young massive stars near Sgr A*, and there is neither a well defined concept of gas density and

temperature at infinity, nor one for the gas capture radius. On the other hand, NIR observations of bright young stars constrain their mass loss rates, wind velocities and stellar orbits^{26,33}. One can then use this information and numerically model gas accretion onto the SMBH.

Three dimensional simulations of wind accretion on Sgr A* were performed by⁵ and³⁸, who randomly positioned \sim a dozen mass-losing stars a few arc-seconds away from Sgr A*. In both cases the stars were at fixed locations, whereas in reality they follow Keplerian orbits around the SMBH. The accretion rate on to Sgr A* predicted by both studies was estimated at $\sim \text{few} \times 10^{-4} M_{\odot} \text{ year}^{-1}$. Finally,³⁷ studied the problem in the approximation that there is an infinite number of wind sources distributed isotropically around Sgr A* in a range of radii. His model yields an accretion rate estimate of $\sim \text{few} \times 10^{-5} M_{\odot} \text{ year}^{-1}$.

We have recently developed and tested a new particle-based approach to this wind accretion problem^{7,8}. The gas dynamics is solved for via the Smoother Particle Hydrodynamics (SPH) formalism using the well tested code Gadget⁴², whereas Sgr A* is modelled as a sink particle. Stars are represented by collisionless particles moving in Sgr A* potential on circular Keplerian orbits, and emitting winds (new SPH particles) with given properties. Further, we include optically thin radiative cooling of the gas.

3.1 Fast winds only

We⁸ first tested one-phase stellar wind problem setting, where all the stellar winds have same velocity of $v_w = 1000$ km/sec, consistent with the shocked gas temperature measured by *Chandra*. The distribution and number of stellar wind sources were varied to study their effects on the results. It was found that the accretion rate onto Sgr A* strongly depends on these factors. Left hand panel of Figure 1 show the accretion rate onto Sgr A* versus time for simulations with 40 stars: (green, solid) fixed in space; (dotted blue) moving on circular orbits isotropically distributed; (red dashed line) on circular orbits for a disk distribution. The variations of stellar positions in time cause significant variations in the accretion rates, whereas for fixed stars the accretion rate is quasi-constant after a steady state is achieved. In addition, the larger the net angular momentum of the stellar orbits, the lower is the accretion rate, reflecting the increased centrifugal support of the gas.

3.2 Fast and slow wind simulations

In reality stellar populations in the immediate vicinity of Sgr A* are diverse. As convincingly shown by³³, a fair fraction of important stellar winds is much slower than 1000 km/sec, i.e. in the range of $v_w \sim 150 - 300$ km/sec. The temperature of the shocked winds scales as v_w^2 , therefore these winds heat up to 'only' $T \lesssim 10^6$ Kelvin, and can cool radiatively in time much shorter than the local dynamical time⁷. It is not clear a priori how these slow cool winds would accrete onto Sgr A* in the presence of mechanically dominant fast winds, and moreover, how the latter will be affected by the former. The results will also likely depend on the distribution of the stellar orbits.

To address these issues, we⁸ set two tests with same overall winds properties but different spatial distributions for stars. In one of the tests, the stars were placed in two perpendicular stellar disks, in a rough accord with the observations¹². In the other, stars were isotropically distributed. The real situation should be somewhere in between these two cases. All (20) stars were losing mass at the same rate, $\dot{M} = 5 \times 10^{-4} M_{\odot}/\text{year}$, but 12 of the stars were assumed to have winds $v_w = 1000$ km/sec, while the remaining 8 had $v_w = 300$ km/sec.

The right panel of Figure 1 shows the resulting accretion rate onto Sgr A* for the two-disks simulation with fast and slow winds. Comparing it to the left panel of the same Figure, we see that the accretion rate of the hot gas (red curve in the right panel) is somewhere in the middle between the isotropic (blue) and disk (red) cases in the left panel. It is however much less

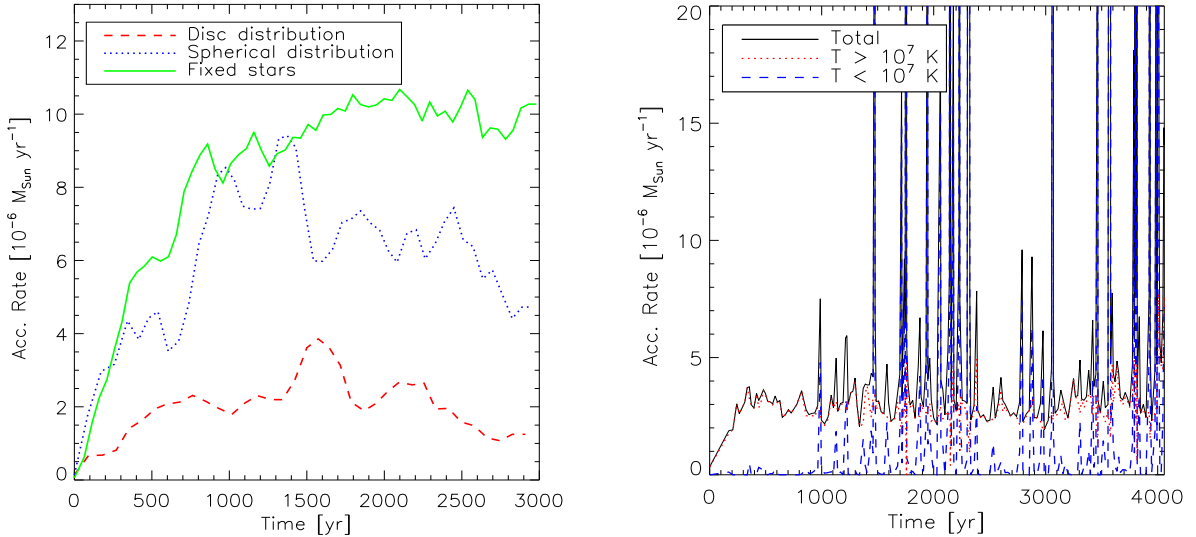


Figure 1: Left: Accretion rates onto Sgr A* in simulations with fast winds. Different lines correspond to different stellar distributions, as marked in the inset. Right: Accretion rate onto Sgr A* for the two-phase wind simulation with two perpendicular stellar disks. The total accretion rate (solid curve) can be broken down onto the quasi-constant hot component (red) and pulse-like cold accretion events (blue).

variable. On the other hand, some of the slow wind gas, radiatively cooled and then compressed into gas filaments and clumps, accretes in short but dramatic accretion episodes (blue line in the right panel).

The left panel of Figure 2 shows the gas column depth, with stars marked in black (for the outer ring perpendicular to the plane of the Figure), or in red symbols (for the inner stellar disk lying in the plane of the Figure). Slow wind gas, cooling radiatively, is compressed by the higher pressure environment created by the hot gas, and forms cool filaments and clumps. Filaments are then sheared, wound up, and form the cool disk. The disk viscous time is too long for the disk material to contribute to accretion onto Sgr A* directly⁷. More likely the disk is destroyed periodically by interactions with frequently passing supernova shells⁸ or infalling ionized gas streamers³⁴. Note that the disk size is smaller than the inner radius of the innermost stellar orbits ($2''$). This is because the disk is made of low angular momentum material: most of both slow and fast wind gas outflow from Sgr A* location.

3.3 Relevance of Sgr A* for energy balance of the gas in the inner Galaxy

The current bolometric X-ray luminosity of Sgr A* is orders of magnitude smaller than that of any one of the dozens of the bright young stars that orbit the SMBH. Thus one may lead to believe that Sgr A* may not be energetically important for the gas energy balance in the inner tens of parsecs of the Galaxy. However, our simulations, while still missing essential ingredients, lead us to dispute such a conclusion. Some of these ingredients are: (i) the presence of a large mass of cold gas³⁴ on elliptical and perhaps even plunging orbits near Sgr A*; (ii) the fact that real stellar populations are more diverse (e.g., AGB stars) than we have assumed; (iii) some of these stars may be on elliptical rather than circular orbits. It is obvious that inclusion of any of these ingredients (which we plan to do in future work) will add further complexity, and a potential for high variability in the accretion rate onto Sgr A*. We believe that, averaged over time scales long compared with Keplerian period at few arcsecond distance away from Sgr A* (e.g. $\sim 10^3$ years), Sgr A* luminosity and mechanical output (jet, gas outflows) are much higher than their present day values.

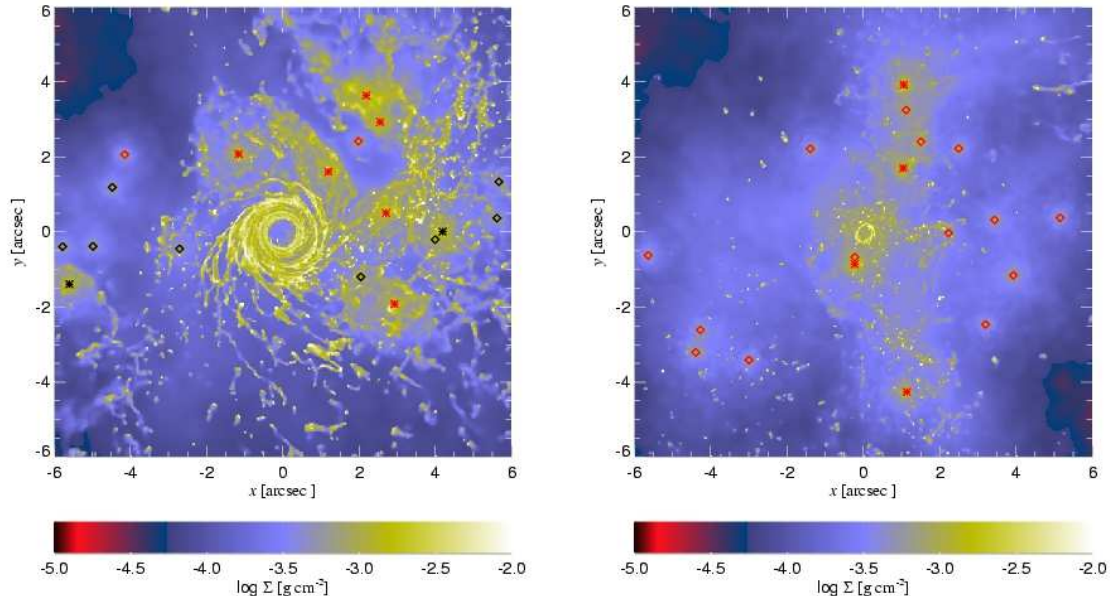


Figure 2: The integrated gas column density for the two simulations that included both slow and fast winds. **Left:** stars are placed into two perpendicular stellar disks. The plane of the cool disk, clearly visible in the panel, nearly coincides with the plane of the innermost stellar disk. **Right:** Same but for stars isotropically distributed. The tiny cool ring orientation is close to that of the innermost slow wind star, and precesses slowly with time.

4 Star formation near Sgr A* in the recent past

Due to dimness of Sgr A*, tens of young massive stars dominate the bolometric energy output of the inner parsec of our Galaxy. Remnants of young massive stars, exploding as supernovae, are also likely to dominate the production of cosmic rays and γ -ray emission in the center of the Galaxy. Therefore, to understand the activity of our Galactic Center we must understand the young stars there. Here we shall concentrate on the more massive brighter young stars mainly located in the two stellar rings^{19,12} as opposed to the less massive but much closer “S-stars” (see^{14,41}). The former are only ~ 4 Million years old. “Normal” modes of star formation at 0.1 pc distances from a SMBH are forbidden due to a huge tidal field of the central object. Star formation in a massive gravitationally unstable accretion disk is a process long considered by theorists^{18,6,15} but not yet observationally confirmed in any of AGN. The young stars in Sgr A* may thus be the first evidence for the ‘exotic’ accretion disc mode of star formation^{19,24,32}. On the other hand, it is also possible that the close young stars were not born there but were rather transported in by dynamical friction, if they earlier were members of a massive young star cluster^{13,17}. It would be extremely important to rule out one or both of these models for the benefit of the general understanding of how stars contribute to the AGN phenomenon.

A successful model for the origin of young stars in Sgr A* will have to explain quantitatively not only the creation of the stars but also their present day orbits. A ring or disc-like configuration of stars thickens with time due to internal N-body evolution, but for disc masses smaller than $M_d \lesssim 3 \times 10^5 M_\odot$ this thickening is slow enough to not contradict the observations³². Such a high mass limit is not constraining for either of the models. ³² also pointed out that because the combined SMBH and young stellar discs gravitational potential is no longer spherically symmetric, stellar orbits will precess. This precession warps initially flat stellar discs (see also³⁰). Stellar discs that end up too strongly warped or thick will contradict the¹¹ results.

We (Nayakshin et al. 2005, in preparation), performed numerical calculations to detail the upper mass limits on the stellar disc masses. First of all, let us estimate the magnitude of the

warping effect. As calculated by⁷ the rate at which a massless accretion disk is warped by a massive stellar ring inclined to the (initially flat) disk at angle β . For radii R much smaller or much larger than the ring radius, R_{ring} , the precession angular frequency $\omega_p(R)$ can be approximated as

$$\frac{\omega_p(R)}{\Omega_K(R)} \approx -\frac{3M_{\text{ring}}}{4M_{\text{BH}}} \cos \beta \frac{R^3 R_{\text{ring}}^2}{[R^2 + R_{\text{ring}}^2]^{5/2}}. \quad (1)$$

Here M_{ring} is the ring mass, assumed to be much smaller than the blackhole mass, M_{BH} , and $\Omega_K(R)$ is the Kepler circular frequency for the disk at radius R . The period of circular motion 3" away from Sgr A* (where most of the bright young stars are found) is around 2 thousand years. Therefore, the stars at this location make about a thousand revolutions in a few million years. Let $\Delta\gamma = \omega_p t$ be the angle on which an annulus of the disk will precess during this time: $\Delta\gamma \sim (M_{\text{ring}}/M_{\text{BH}}) \times 1000$. Very approximately, the disk warping will be noticeable when $\Delta\gamma \sim 1$. Thus mass ratios ($M_{\text{ring}}/M_{\text{BH}}$) in excess of 10^{-3} or so may lead to warping of the stellar disks in Sgr A*.

Equation 1 depends on angle β , and would also depend on eccentricity of a stellar orbit if it were not assumed to be zero in the derivation. Therefore, if initial distributions of stellar eccentricities and inclinations (with respect to the other disk) are different for the two competing models, they will be warped/thickened by different amounts. This is indeed the case. Stars are expected to be born on nearly circular Keplerian orbits³², i.e. with eccentricity $e \sim H/R \ll 1$, for star formation in a self-gravitating disc (also, stars are unlikely to drift significantly in the radial direction due to the star-gas dynamical friction). On the other hand,²⁰ have recently demonstrated that, due to a repetitive interaction with the IMBH, stars just peeled off the IMBH-star cluster gain a substantial eccentricity to their orbits. Even for the case of the circular IBMH inspiral, stars acquire a mean eccentricity of $e \approx 0.5$. We may thus expect different mass limits for the two models of the origin of the young stars near Sgr A*. To be quantitative, we perform numerical simulations and do a reduced χ^2 fit to compare the simulated discs to the actual ones.

4.1 Numerical method nad sample results

To follow stellar orbits, we use the N-body package "NEMO" with the orbit integrator⁹ *gyrfal-cON*. The code calculates gravitational interaction of all the particles and updates their velocities and positions. The masses of the stars in a given simulation are typically chosen to be in the range expected of massive stars, e.g. $M_* = M_{\text{disk}}/N_{\text{disk}} = 20 M_{\odot}$, for typical numbers below. We use between few hundred to few thousand particles for each of the two stellar systems.

To set up the problem, we shall rely on the gross results of¹¹, and the more recent analysis of the data by¹⁰. For convenience, we shall refer to the clock-wise rotating system in the GC as a disk, and the counter clock-wise system as a ring. To model the "disk", we start with stars initially in a disk with the radial extent from $R_{\text{in}} = 2''$ to $R_{\text{out}} = 5''$. The observed counter clock-wise system contains fewer stars and it is harder to assign the radial extent for this system. We used two plausible guesses for the ring, therefore: one is a ring between $R_{\text{in}} = 4''$ and $R_{\text{out}} = 5''$, and the other is a ring between $R_{\text{in}} = 5''$ and $R_{\text{out}} = 7''$. The initial inclination between the two systems is set at $\beta = 113^\circ$ ¹¹.

The simulations were ran until time $t \approx 3$ Million years. At the end of a simulation, we fit the two stellar systems by a plane in velocity space. A plane is characterised by vector \vec{n} ortogonal to the plane and normalized to unity, $\vec{n}^2 = 1$. The best fitting planes are found via the reduced χ^2 method⁹ for both of the two stellar systems. For simplicity we assume that velocity errors are isotropic, i.e. each component is equal to $\sigma/\sqrt{3} \approx 40$ km/sec, where $\sigma = 70$ km/sec.

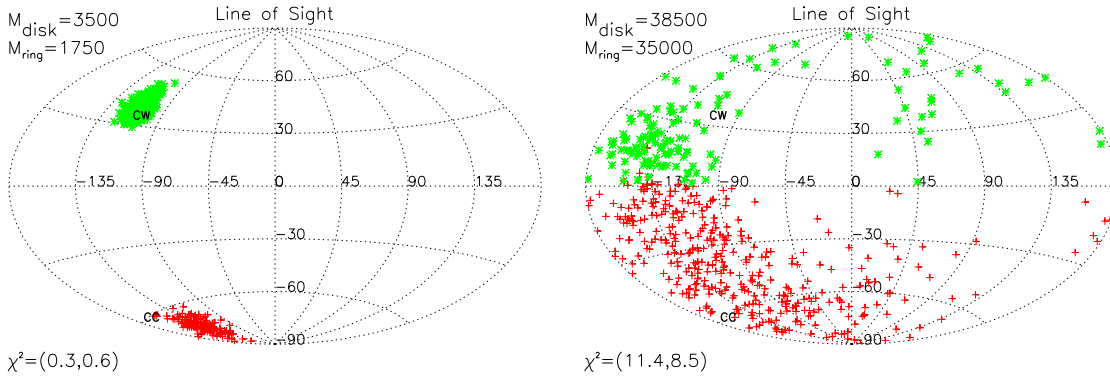


Figure 3: Angular momentum directions for individual stars in the two disks at the end of simulations. Initially the stars in the disks were on circular orbits with angular momentum directions given by the positions 'CW' and 'CC' **Left:** A simulation in which both clock-wise (disk) and counter clock-wise (ring) systems have relatively low masses, as indicated in the right upper corner of the panel. Such masses produce very weak warping of the disks, and thus small values of the reduced χ^2 pair (lower left corner). This simulation does not violate observational constraints. **Right:** Same but for much higher values of M_{disk} and M_{ring} . The stars orbits precess very strongly and the disks are actually hard to separate in this case. Both stellar systems produce χ^2 values few times larger than the values observed. Such high disk stellar masses are strongly rejected.

We illustrate results with two representative runs performed assuming circular initial orbits. The results of these two simulations are presented in Figure 3, which shows the two angles describing the directions of the angular momentum vectors of all of the stars used in the simulations (these coordinates were recently used by¹⁰). The latitude shows the inclination of the direction to the line of sight, whereas the longitude shows the position angle on the sky. A star rotating exactly in the plane of the sky clock-wise would end up on the north pole in this plot. Stars that belong to the clock-wise disk (marked 'CW' in the Figure) are marked with symbols in green, and the counter clock-wise ('CC' system) is marked in red.

In the simulation shown in the left panel, the masses of the stellar systems are quite small, e.g. $M_{\text{disk}} = 3.5 \times 10^3 M_{\odot}$ and $M_{\text{ring}} = 1.75 \times 10^3 M_{\odot}$, respectively. Precession of stellar orbits for both the disk and the ring is minimal, and the resulting reduced χ^2 fits to the stellar planes are much better than they are in reality (2.5 and ~ 4.0 , respectively). Such small disk masses are consistent with observations. The next test, shown in the right panel of the same Figure, is a simulation with the disk and ring masses both about $\sim 3 \times 10^4 M_{\odot}$. The stellar systems become warped so much that it is hard to separate them out, strongly contradicting the observations¹¹.

4.2 Summary of results

By calculating a grid of models within a broad range of disk masses, we estimated that for the circular initial stellar orbits, the maximum total stellar masses for the systems are: $M_{\text{disk}} \simeq 2 \times 10^4$ and $M_{\text{ring}} \simeq 10^4$, for the clock-wise and the counter clock-wise systems, respectively. Interestingly, the minimum mass of the *gaseous* disk needed to initiate gravitational collapse of a standard accretion disk³² is a factor of 2-4 smaller than these upper limits. Thus, even if all of the gass mass ended up collapsing and accreting onto the stars, the accretion disk model could be made consistent with the present day orbits of young stars in Sgr A*.

For the simulations with initial stellar velocities distributed as expected for a *circular* inspral of a cluster²⁰, we find that the stellar disks become warped understandably faster (because there is a greater variety of stellar orbits inside of each of the stellar systems). The limits on the stellar mass of the disks are then reduced by a factor of $\simeq 2$. Now, the initial mass of the observed young stars may be estimated as $\sim 3 \times 10^3 M_{\odot}$, and the normal galactic IMF would

suggest that the total mass of young stars (including Solar-mass stars), would be in the range of $\sim \text{few} \times 10^4 M_\odot$ at least¹⁷. However, the IMF may be very top-heavy in this case²⁵, and besides the lower mass stars may be effectively peeled off the sinking cluster at much greater radii¹⁶. Therefore the circular cluster inspiral also passes the ‘disk warping’ test.

However, while we have not yet studied the elliptical cluster inspiral case, we are confident that the upper mass limits on stellar mass are likely to be reduced further and would start to conflict with the minimum stellar mass in the observed massive stars. In addition, at least the stars in the clock-wise stellar system appear to be on circular rather than on strongly elliptical orbits (R. Genzel and T. Paumard, private communication). Therefore it appears that only a circular cluster infall model may be viable.

Finally, we should remember that the **two** stellar systems in the GC center require two star formation events, and for the cluster infall scenario this means two clusters with initial stellar masses in the range of $10^5 - 10^6$ Solar masses^{17,16}, and of course a factor of few more in the initial molecular cloud mass prior to star formation. In my opinion this is a rather unlikely situation then contrasted with the accretion disk model which requires gas masses of just around $10^4 M_\odot$ for both star formation episodes.

5 Conclusions

We have addressed three separate topics that are arguably of the greatest current interest to researchers of Sgr A*. First of all, quiescent multi-waveband emission of Sgr A* indicates that the accretion flow is comprised of very hot, low density, two-temperature plasma. Electrons are predominantly thermal and are much cooler than ions. An energetically weak non-thermal population of electrons may be present. The X-ray and NIR flares of Sgr A* are likely produced by this populations which gains prominence during flares. Detailed physics of the collisionless plasma in quiescence and during flares is still missing but is a subject of current research. Close stellar approaches of bright young stars may be used to put constraints on some of this physics.

We then discussed numerical simulations of stellar wind accretion onto Sgr A*. The more realistic slow and fast wind simulations^{7,8}, and some further preliminary work indicates that accretion rate onto Sgr A* may be strongly time variable on time scales of stellar orbits of important mass losing stars, e.g. hundreds to thousands of years. The time-averaged radiative and mechanical energy (e.g. jet) outputs of Sgr A* are thus likely to be much greater than their current respective values. Sgr A* may be an important contributor to the energy balance of the gas in the inner tens of parsecs of the Galaxy, a not trivial conclusion given the current miserable state of Sgr A*.

On the issue of recent star formation, we have shown how constraints from stellar dynamical evolution can be used to set limits on the time-average mass of the two stellar systems observed in the GC. These limits yield total stellar masses no larger than $\lesssim 10^4 M_\odot$, with limits becoming tighter when eccentricity of initial stellar orbits is increased. The star formation in accretion disk model comfortably passes within these stellar dynamical constraints. The infalling cluster model also satisfies the constraints as long as the eccentricity of cluster inspiral is not too large. However, considering this limitation, and the fact that initial gas masses needed to account for the observed young stars in this model are measured in millions of Solar masses, and require two independent (very massive) cluster infall episodes, I argue that this model should be viewed as an unlikely one.

Acknowledgments

Jorge Cuadra has significantly contributed to this work. Walter Dehnen provided the most recent version of his N-body code and advice on using it. Reinhard Genzel and Thibaut Paumard are

thanked for many useful discussions and access to their yet unpublished results. I am also very thankful to conference organizers for inviting me to this exciting meeting, and to Jacques Dumarchez in particular for patience while I was finishing this paper.

References

1. Baganoff, F.K., et al., ApJ **591**, 891 (2003)
2. Baganoff, F. K., et al. 2001, Nature, 413, 45
3. Blandford, R.D., & Begelman, M.C., MNRAS **303**, L1 (1999)
4. Bower, G. C., Wright, M. C. H., Falcke, H., & Backer, D. C. 2003, ApJ, 588, 331
5. Coker, R. & Melia, F. ApJL **488**, L149 (1997)
6. Collin, S., & Zahn, J. 1999, A&A, 344, 433
7. Cuadra, J., Nayakshin, S., et al., to appear in MNRAS, 2005 (astro-ph/0502044)
8. Cuadra, J., Nayakshin, S., et al., submitted to MNRAS, 2005 (astro-ph/0505382).
9. Dehnen, W. 2000, ApJL, 536, L39
10. Eisenhauer, F., et al. 2005, submitted to ApJ (astro-ph/0502129).
11. Genzel, R., et al., Nature **425**, 934 (2003)
12. Genzel, R., et al., ApJ **594**, 812 (2003)
13. Gerhard, O. 2001, ApJL, 546, L39
14. Ghez, A.M., et al., ApJL **586**, L127 (2003)
15. Goodman, J. 2003, MNRAS, 339, 937
16. M. A. and Rasio, F. A., 2005, to appear in ApJ (astro-ph/0412452).
17. Kim, S. S., Figer, D. F., & Morris, M. 2004, ApJL, 607, L123
18. Kolykhalov, P. I., & Syunyaev, R. A. 1980, Soviet Astronomy Letters, 6, 357
19. Levin, Y., & Beloborodov, A. M. 2003, ApJL, 590, L33
20. Levin, Y., Wu, A. S. P., & Thommes, E. W. 2005, submitted to ApJ (astro-ph/0502143)
21. Liu, S., & Melia, F. 2001, ApJL, 561, L77
22. Mahadevan, R., & Quataert, E. 1997, ApJ, 490, 605
23. Markoff, S., Falcke, H., Yuan, F., & Biermann, P. L. 2001, A&A, 379, L13
24. Milosavljević, M., & Loeb, A. 2004, ApJL, 604, L45
25. Morris, M. 1993, ApJ, 408, 496
26. Najarro, F., Krabbe, et al. 1997, A&A, 325, 700
27. Narayan, R., & Yi, I. 1994, ApJL, 428, L13
28. Narayan, R. 2002, in Lighthouses of the Universe: The Most Luminous Celestial Objects and Their Use for Cosmology Proceedings of the MPA/ESO/USM (Springer, 2002)
29. Nayakshin, S., Cuadra, J., & Sunyaev, R. A&A **413**, 173 (2003)
30. Nayakshin, S. 2005, MNRAS, 359, 545
31. Nayakshin, S. A&A **429**, L33 (2005)
32. Nayakshin, S., & Cuadra, J. 2005, to appear in A&A (astro-ph/0409541)
33. Paumard, T., Maillard, J. P., Morris, M., & Rigaut, F. 2001, A&A, 366, 466
34. Paumard, T., Maillard, J.-P., & Morris, M. 2004, A&A, 426, 81
35. Porquet, D., et al. 2003, A&A, 407, L17
36. Quataert, E., & Gruzinov, A. 2000, ApJ, 539, 809
37. Quataert, E. 2004, ApJ, 613, 322
38. Rockefeller, G., Fryer, C. L., Melia, F., & Warren, M. S. 2004, ApJ, 604, 662
39. Shakura, N. I., & Sunyaev, R. A. 1973, A&A, 24, 337
40. Shapiro, S. L., Lightman, A. P., & Eardley, D. M. 1976, ApJ, 204, 187
41. Schödel, R., et al. 2002, Nature, 419, 694
42. Springel, V., Yoshida, N., & White, S. D. M. 2001, New Astronomy, 6, 79
43. Terashima, Y., Iyomoto, N., Ho, L. C., & Ptak, A. F. 2002, ApJS, 139, 1

44. Yuan, F., Quataert, E., & Narayan, R. 2003, *ApJ*, 598, 301